Journal of Digital Imaging (2021) 34:637–646
https://doi.org/10.1007/s10278-021-00457-y

Rapid Assessment of Acute Ischemic Stroke by Computed Tomography Using Deep Convolutional Neural Networks

Chung-Ming Lo[1,2] · Peng-Hsiang Hung[1,3] · Daw-Tung Lin[4]

Received: 8 May 2020 / Revised: 10 March 2021 / Accepted: 27 April 2021 / Published online: 7 May 2021

Abstract

Acute stroke is one of the leading causes of disability and death worldwide. Regarding clinical diagnoses, a rapid and accurate procedure is necessary for patients suffering from acute stroke. This study proposes an automatic identification scheme for acute ischemic stroke using deep convolutional neural networks (DCNNs) based on non-contrast computed tomographic (NCCT) images. Our image database for the classification model was composed of 1254 grayscale NCCT images from 96 patients (573 images) with acute ischemic stroke and 121 normal controls (681 images). According to the consensus of critical stroke findings by two neuroradiologists, a gold standard was established and used to train the proposed DCNN using machine-generated image features. Including the earliest DCNN, AlexNet, the popular Inception-v3, and ResNet-101 were proposed. To train the limited data size, transfer learning with ImageNet parameters was also used. The established models were evaluated by tenfold cross-validation and tested on an independent dataset containing 50 patients with acute ischemic stroke (108 images) and 58 normal controls (117 images) from another institution. AlexNet without pretrained parameters achieved an accuracy of 97.12%, a sensitivity of 98.11%, a specificity of 96.08%, and an area under the receiver operating characteristic curve (AUC) of 0.9927. Using transfer learning, transferred AlexNet, transferred Inception-v3, and transferred ResNet-101 achieved accuracies between 90.49 and 95.49%. Tested with a dataset from another institution, AlexNet showed an accuracy of 60.89%, a sensitivity of 18.52%, and a specificity of 100%. Transferred AlexNet, Inception-v3, and ResNet-101 achieved accuracies of 81.77%, 85.78%, and 80.89%, respectively. The proposed DCNN architecture as a computer-aided diagnosis system showed that training from scratch can generate a customized model for a specific scanner, and transfer learning can generate a more generalized model to provide diagnostic suggestions of acute ischemic stroke to radiologists.

Keywords Acute ischemic stroke · Computed tomography · Convolutional neural networks

Introduction

According to World Health Organization statistics, stroke is the most common form of cerebrovascular disease among adults, is one of the leading causes of death, and the major cause of permanent disability globally. Every two seconds, someone suffers a stroke, which results in approximately 6.24 million deaths worldwide each year [1]. Stroke patients are at high risk of recurrence, which increases from 3% (after 30 days) to 40% (after 10 years) [2]. Additionally, the Global Burden of Disease reports that up to 11 million stroke cases occur in young adults aged 20~64 years [3]. Stroke is a brain injury that induces physical impacts, such as limb impairment, dementia, aphasia, and cognitive abnormalities [4, 5], which impair patients' independence. The required expenditures for medical resources and family burdens are

Peng-Hsiang Hung and Daw-Tung Lin contributed equally to this work

✉ Peng-Hsiang Hung
sacbusec175@gmail.com

✉ Daw-Tung Lin
dalton@mail.ntpu.edu.tw

[1] Graduate Institute of Biomedical Informatics, College of Medical Science and Technology, Taipei Medical University, Taipei, Taiwan

[2] Graduate Institute of Library, Information and Archival Studies, National Chengchi University, Taipei, Taiwan

[3] Department of Radiology, Mackay Memorial Hospital, No. 92, Sec. 2, Zhongshan N. Rd., 10449 Taipei City, Taiwan

[4] Department of Computer Science and Information Engineering, National Taipei University, 151 University Rd., Taipei 237 Sanshia, Taiwan

enormous. Therefore, timely stroke recognition and treatment are urgently needed to reduce brain tissue injury as much as possible.

Stroke caused by disruption of blood supply to the brain can be classified into either rupture or blockage of blood vessels, namely, hemorrhagic and ischemic stroke, respectively [6]. Ischemic stroke is by far the most common type (up to 80%) worldwide [7]. The main cause is large vessel occlusion due to either an arterial or cardiac embolism [8]. The primary goal of critical treatment in the acute phase of ischemic stroke is to recover the supply of blood perfusion. Good clinical outcomes were correlated with early vessel recanalization [9, 10]. The correct use of treatment highly depends on an accurate diagnosis of acute ischemic stroke; therefore, a rapid and reliable imaging examination is necessary for subsequent treatment.

Non-contrast computed tomography (NCCT) and magnetic resonance imaging (MRI) are routinely used to diagnose ischemic stroke [11]. NCCT is a fast and readily available diagnostic tool for emergency situations and is used to detect cerebral hemorrhage (a contraindication to thrombolytic therapy) or other mimics of acute stroke. Diffusion-weighted imaging is a highly sensitive MRI technique that provides reliable information on acute cerebral ischemia [12]. Compared to NCCT, MRI is less accessible and more limited by patient intolerance, contraindications, and a long examination duration. Consequently, NCCT remains the first-line imaging modality for identifying ischemia extent in the brain parenchyma [13]. Nevertheless, these findings are present in fewer than 50% of cases [14]. Erroneous interpretations, such as sulcal effacement and inconsistent scanning protocols, limit the sensitivity of NCCT. In the literature, NCCT has a sensitivity of 57~71% within 24 h and only 12% in the first 3 h [15, 16].

With the development of image processing, computer-aided diagnosis (CAD) systems based on quantitative image features and machine learning techniques can achieve better efficiency and accuracy [17, 18], and the use of CAD in diagnosing acute ischemic stroke by NCCT can meet clinical needs. CAD systems are quantitative, efficient, and consistent; therefore, CAD systems have been proposed to improve diagnostic quality. For example, textural features are used to evaluate liver cirrhosis at an early stage based on ultrasound images [19]. Shape features are used to automatically detect pulmonary nodules in CT imaging [20] and detect masses and microcalcifications on mammograms [21]. Previous CAD systems used handcrafted shape, intensity, and textural features that were manipulated by human experts; however, selecting and implementing relevant features are complicated and may be biased. Deep convolutional neural networks (DCNNs) are a better approach to automatically generate and combine image features. DCNNs with multiple convolutional layers can extract as much information as possible from images, which are automatically processed with several types of filters and learn to recognize features at differing spatial levels [22]. Prior literature showed that the performance of DCNN in diagnosing diabetic retinopathy and skin cancer outperformed specialized expertise with an area under the receiver operating characteristic curves (AUC) for accuracy of 0.96–0.99 [23–25]. In this study, DCNN as a CAD system was proposed to diagnose acute ischemic stroke on NCCT images to provide an efficient and accurate diagnostic suggestion for clinical use. Additionally, NCCT image datasets were collected from different scanners and institutions for performance validation to evaluate the generalizability of the trained model.

Materials and Methods

Study Participants and Image Acquisition

The study protocol was reviewed and approved by our institutional review board (No. 17MMHIS133). The collected NCCT image datasets were from two institutions. As shown in Fig. 1, the main dataset from institution A was used for conventional model building. The dataset was separated into a training set and a test set under tenfold cross validation for evaluation. Additionally, the image dataset from institution B was also used for an independent test to verify model performance regarding data from different protocols, scanners, and institutions.

From January 2017 to December 2019, the image dataset from institution A contains a total of 1254 NCCT slices, including 573 stroke slices and 681 normal slices from 96 acute ischemic stroke patients and 121 normal control patients. Among the 96 stroke patients, a baseline NCCT was performed within a mean of 127 min and a median of 113 min after the time of last known wellness. Images reconstructed in the axial CT were acquired using routine brain window settings (width, 100 HU; center, 35 HU) to generate 512 × 512 images (Fig. 2a). Between January 2018 and October 2019, the image dataset from institution B consisted of 108 stroke slices and 117 normal slices, which were extracted from 50 acute ischemic stroke patients and 58 normal control patients for independent model testing. Among the 50 stroke patients, a baseline NCCT was performed within a mean of 121 min and a median of 109 min after the time of last known wellness. Images reconstructed in the axial CT were acquired using routine brain window settings (width, 90 HU; center, 40 HU) to generate 512 × 512 images (Fig. 2b). Patients with negative findings on neurological examination and no structural abnormalities on NCCT were recruited as normal controls. Forty-two patients with vertebrobasilar artery occlusion ($n = 13$), arrival time > 6 h ($n = 24$), and motion artifacts ($n = 5$) were excluded. Patient characteristics are listed in Table 1.

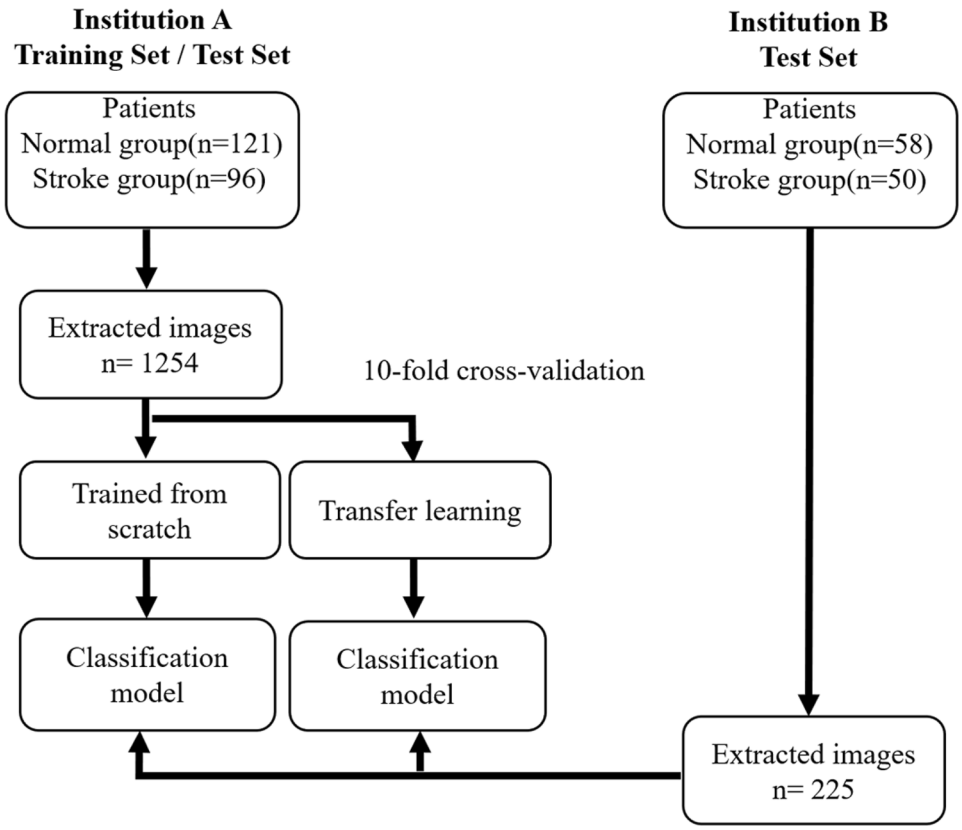

Fig. 1 The flowchart and datasets used in the experiments for the establishment and evaluation of DCNN models

Due to the lack of MRI in experimental institutions, the standard practice during the acute period is a baseline NCCT accompanied by multiphase CT angiography (CTA) for diagnosis. Acute status means that the patients presented within 6 h after the onset of stroke symptoms. This period was chosen because NCCT is performed quickly to provide suggestions for appropriate treatment and triage. A multiphase CTA interpretation was then used for rapid identification and vessel evaluation before treatment. Thus, only patients with acute ischemic stroke with intracranial internal carotid artery (ICA) occlusion or middle cerebral artery (MCA) territory occlusion on CTA were included. All CTA scans were performed from the beginning of the aortic arch to the vertex of the arterial phase. The remaining two phases are from the skull base to the vertex in the equilibrium venous and late venous phases in the whole brain. Assessment of pial arterial filling in multiphase CTA was used as the reference standard (Fig. 2c) and to aid in planning for endovascular revascularization (Fig. 2d).

Multislice CT scanners were obtained from two manufacturers with a tube voltage of 120 kVp and automatic tube current modulation. The Siemens scanner (Somatom Definition AS) had a slice thickness = 5 mm, helical pitch = 1.0, and gantry rotation time = 1.00 s. The Toshiba scanner (Aquilion Prime) had a slice thickness = 4 mm, helical pitch = 0.6, and gantry rotation time = 0.75 s. The coverage range was from the skull base to the vertex with continuous axial slices parallel to the orbitomeatal line. According to the multiphase CTA and reperfusion therapy observations, each NCCT image was assigned a standard diagnosis based on consensus of stroke findings by two certified neuroradiologists. Figure 2e shows NCCT examples from the different scanners accompanied by multiphase CTA.

DCNN Architectures

Recent advances in deep learning have garnered attention with respect to pattern recognition of images. DCNN builds on deep learning using multiple network layers to increase performance, such as AlexNet [26], which consists of five convolutional layers, three max pooling layers, and two fully connected layers. As a brief overview of the mechanics behind DCNNs (Fig. 3a), convolutional layers are the processes that featurize images, thereby converting raw input images into useful parameters that can be used to train subsequent models. This process is fully automated and culminates in an output layer that can be used to formulate a prediction. Each convolutional layer uses a rectified linear unit activation function to achieve faster convergence. Max pooling layers partition feature maps and extract maximal values. To prevent overfitting, a dropout layer is also used. The last fully connected layer with a softmax classifier

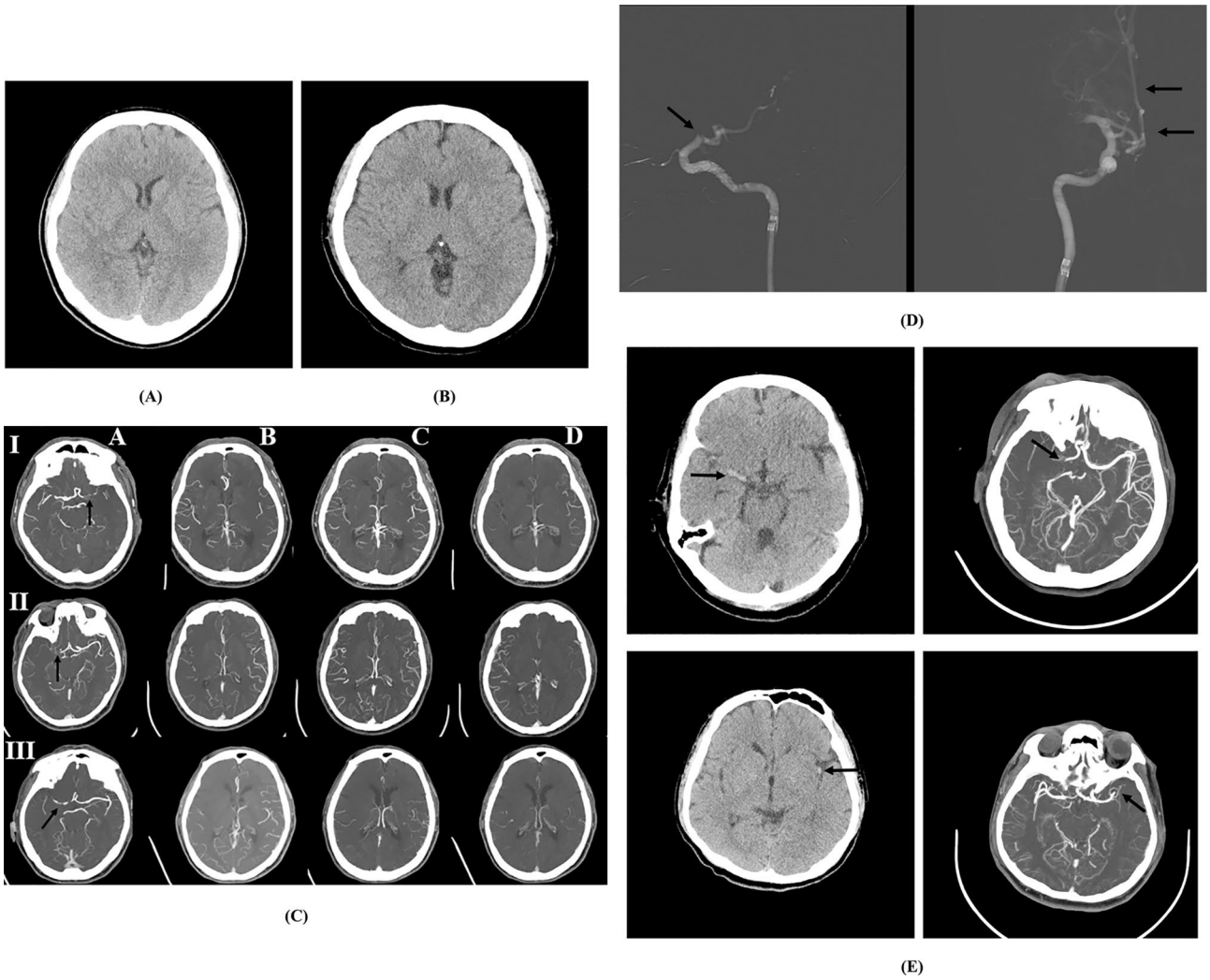

Fig. 2 Illustrative example of NCCT and accompanying imaging examinations. NCCT images from two examinations showing two patients who had no structural abnormalities, indicating normal brain parenchyma density, normal ventricular system, and centrally located midline structures from a **a** Siemens and **b** Toshiba scanner, respectively. **c** Schematic of collateral circulations. Left to right (**a**–**d**) shows the site of occlusion (arrow), arterial, equilibrium venous, and late venous phase, with rows (I–III) showing good collaterals, intermediate collaterals, and poor collaterals. **d** A 73-year-old man with acute infarcts presented within 3 h. Pial arterial filling is moderate, with a delay of two phases indicating intermediate filling compared with the contralateral side. After administration of intravenous recombinant tissue plasminogen activator (rt-PA), the patient had no neurologic improvement, and therefore was taken for endovascular intervention. Due to the right ICA with the occlusion site around the distal cavernous to the supraclinoid segment (arrow), intra-arterial thrombectomy was performed under the impression of focal thrombus to achieve revascularization (arrows). **e** The top row shows NCCT obtained within 4.5 h in a 68-year-old woman with left hemiplegia that was diagnosed by a hyperdense vessel sign in the right proximal MCA (arrow). The arterial phase showed the apparent absence of a right M1 segment embolic occlusion (arrow). The bottom row shows NCCT (5-h evolution) in a 54-year-old man with right-sided weakness diagnosed with the dot sign in the left MCA territory (arrow), loss of left-sided gray–white matter differentiation, and obscuration of the left basal ganglia. The arterial phase showed a filling defect of the left proximal M2 segment thrombus occlusion (arrow)

classifies the slices into normal or stroke. Constructing an effective DCNN from scratch requires a large training dataset. With limited training data, transfer learning retains the initial pretrained model weights and extracts image features via fine-tuning of the network layers (Fig. 3b). Transferred DCNNs have been used in medical diagnosis, such as the assessment of wrist fractures and shoulder lesions, with AUCs of 0.95 and 0.96, respectively [27, 28]. Other studies classified pneumonia in chest radiographs and obtained an AUC between 0.853 and 0.931 [29, 30]. More DCNN architectures were developed to obtain higher accuracy or efficiency, including Inception-v3 [31] and ResNet101 [32]. Inception-v3 is a modification of GoogLeNet. The proposed inception blocks have a multipath structure for the generous

Table 1 Stroke findings in different examinations for emergent management of acute ischemic stroke

Dataset from institution A	No. patient	NCCT(lesion laterality)	Multiphase CTA(pial arterial filling evaluation)
Normal	121	N/A	N/A
Intracranial ICA occlusion	40	39 right side	18 Good collaterals
MCA territory	56	51 left side 6 bilateral side	55 Intermediate collaterals 23 Poor collaterals
Dataset from institution B			
Normal	58	N/A	N/A
Intracranial ICA occlusion	23	21 right side	9 Good collaterals
MCA territory	27	25 left side 4 bilateral side	28 Intermediate collaterals 13 Poor collaterals

N/A not applicable, *NCCT* non-contrast CT, *CTA* CT angiography, *ICA* internal carotid artery, *MCA* middle cerebral artery

use of dimensional reduction and parallel structures of the inception modules, resulting in a decrease in computational complexity. ResNet-101 uses skip connections by fitting residual blocks instead of full feature transformation. Adding skip connections where the gradients can skip and flow better throughout the network. To assess the performances of different architectures for stroke diagnosis, the AlexNet, transferred AlexNet, transferred Inception-v3, and transferred ResNet-101 models were compared. Stochastic gradient descent with a momentum optimizer was used. Output data were compared with the training data, and the error was back-propagated to update parameters in the DCNN so that the error between the output data and training data was minimal. The minimum batch size was 64, the learning rate was 0.001, and 100 epochs were used in the cross-entropy loss function as training batches reached a low plateau toward the end of training (Fig. 4). The performances were quantitatively determined via the accuracy, sensitivity, specificity, and AUC.

Results

The performances of the four DCNN models using the dataset from institution A are listed in Table 2. Ten-fold cross-validation was applied to evaluate how the model could be generalized to an independent dataset. With tenfold cross-validation, the dataset was first randomly partitioned into 10 equal folds. Then, 10 iterations of training and validation were performed, where in each iteration, nine folds were used for training and a different fold of data was held out for validation.

AlexNet achieved an accuracy of 97.12%, a sensitivity of 98.11%, and a specificity of 96.08%, which were better than those of the transferred AlexNet: 90.49%, 96.98%, and 83.73%, respectively. Regarding transferred Inception-v3 and transferred ResNet-101, the accuracy, sensitivity, and specificity were 94.62%, 93.98%, and 95.29%, and 95.49%, 94.36%, and 96.67%, respectively. With respect to the trade-offs between the sensitivity and specificity, the observed AUC of AlexNet was 0.9927, which was also higher than transferred AlexNet (0.9895), transferred Inception-v3 (0.9889), and transferred ResNet-101 (0.9897) (Fig. 5).

Table 3 shows the independent test results regarding the dataset from institution B. AlexNet showed 60.89% accuracy, 18.52% sensitivity, and 100% specificity. Transferred AlexNet achieved 81.77% accuracy, 62.04% sensitivity, and 100% specificity. Transferred Inception-v3 achieved 85.78% accuracy, 75% sensitivity, and 95.73% specificity. Transferred ResNet-101 achieved 80.89% accuracy, 61.11% sensitivity, and 99.15% specificity. With respect to the example of misclassified cases in Fig. 6, tissues suffering from ischemia have complex anatomical structures and the pathologic findings may confuse the DCNNs.

Discussion

NCCT is used to rapidly identify parenchymal findings of ischemic stroke in the acute stage. When ischemia occurs, cytotoxic edema (intracellular) in the affected parenchyma can lead to tissue hypoattenuation on NCCT. NCCT signs may be subtle to the human eye, especially in the hyperacute stage, and there is substantial interrater variability in diagnosing early ischemic changes, ranging from 20 to 69% sensitivity with a very restricted time window [33, 34]. The reliability of an imaging finding is a critical parameter that determines its clinical utility.

In addition, these early signs are not useful for distinguishing between an ischemic penumbra and a core infarction. The Alberta Stroke Program Early CT Score (ASPECTS), an objective method to evaluate the extent of ischemia and prognosis that is widely used, was developed to standardize the analysis of early ischemic signs with

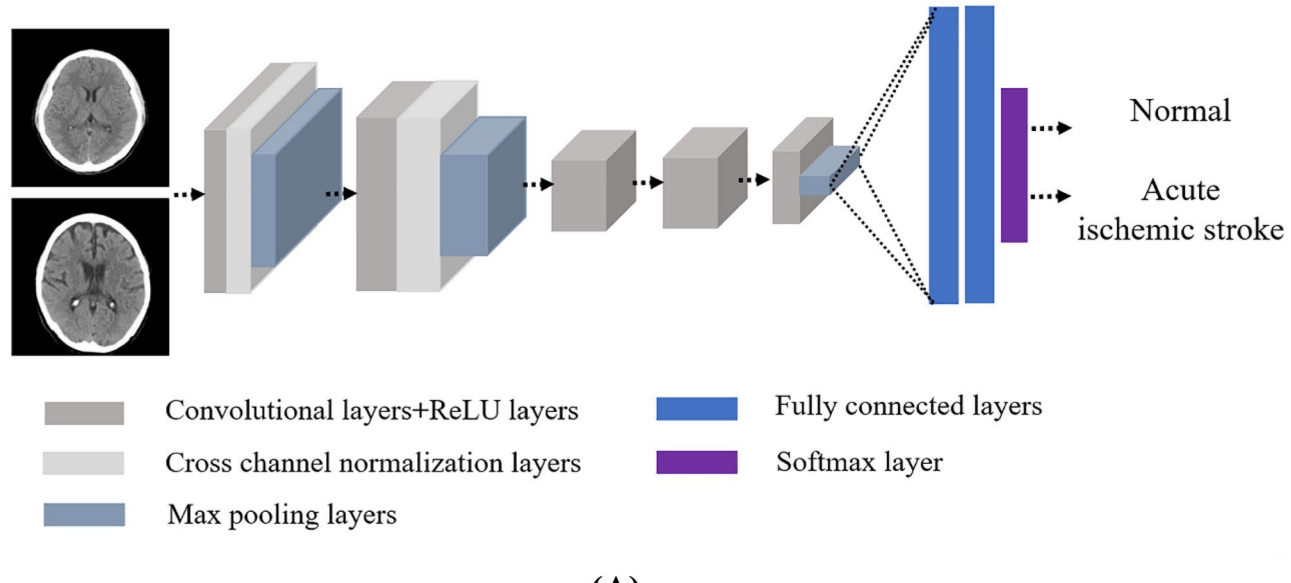

(A)

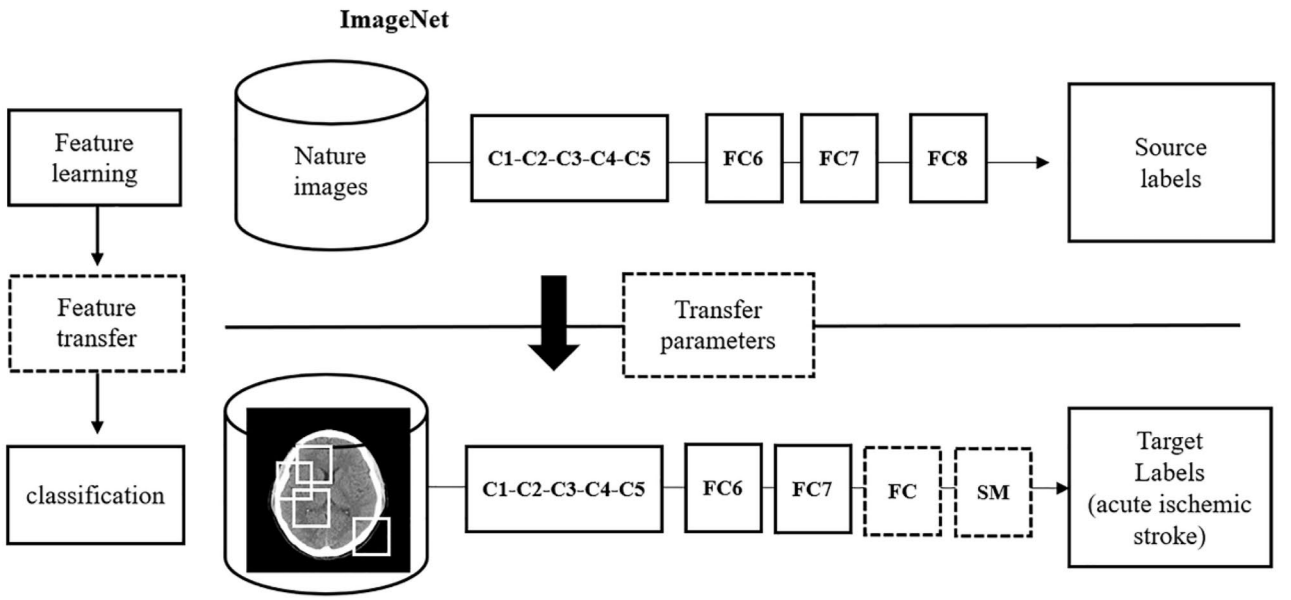

(B)

Fig. 3 Illustration of the basic DCNN for acute ischemic stroke image classification. **a** A schematic representation of a convolutional neural network. **b** Layer structures of the modified AlexNet architectures and transfer learning (dotted line) used in the experiment. C convolutional layer, FC fully connected layer, SM softmax loss function

excellent interobserver reliability, but is too time-consuming for radiologists to perform in clinical settings [35]. The interobserver reproducibility of ASPECTS varies depending on the reader's experience, the amount of reader training, stroke knowledge, and stroke onset-to-imaging time. Reader inexperience and a lack of rigorous ASPECTS training were highlighted as potential causes of suboptimal interobserver agreement. Yong et al. [36] reported limits of ASPECTS as a predictor, such as small hypodensities (lacunar infarct) and age-related white matter hypodensities. Prior reports described that ischemic stroke detection within 12 h varied with pretreatment NCCT ASPECTS, including the location of the arterial occlusion, the time of stroke onset, and image acquisition [37, 38]. Furthermore, reperfusion therapy in ischemic stroke increases the risk of intracerebral hemorrhage. Symptomatic intracerebral hemorrhage occurs

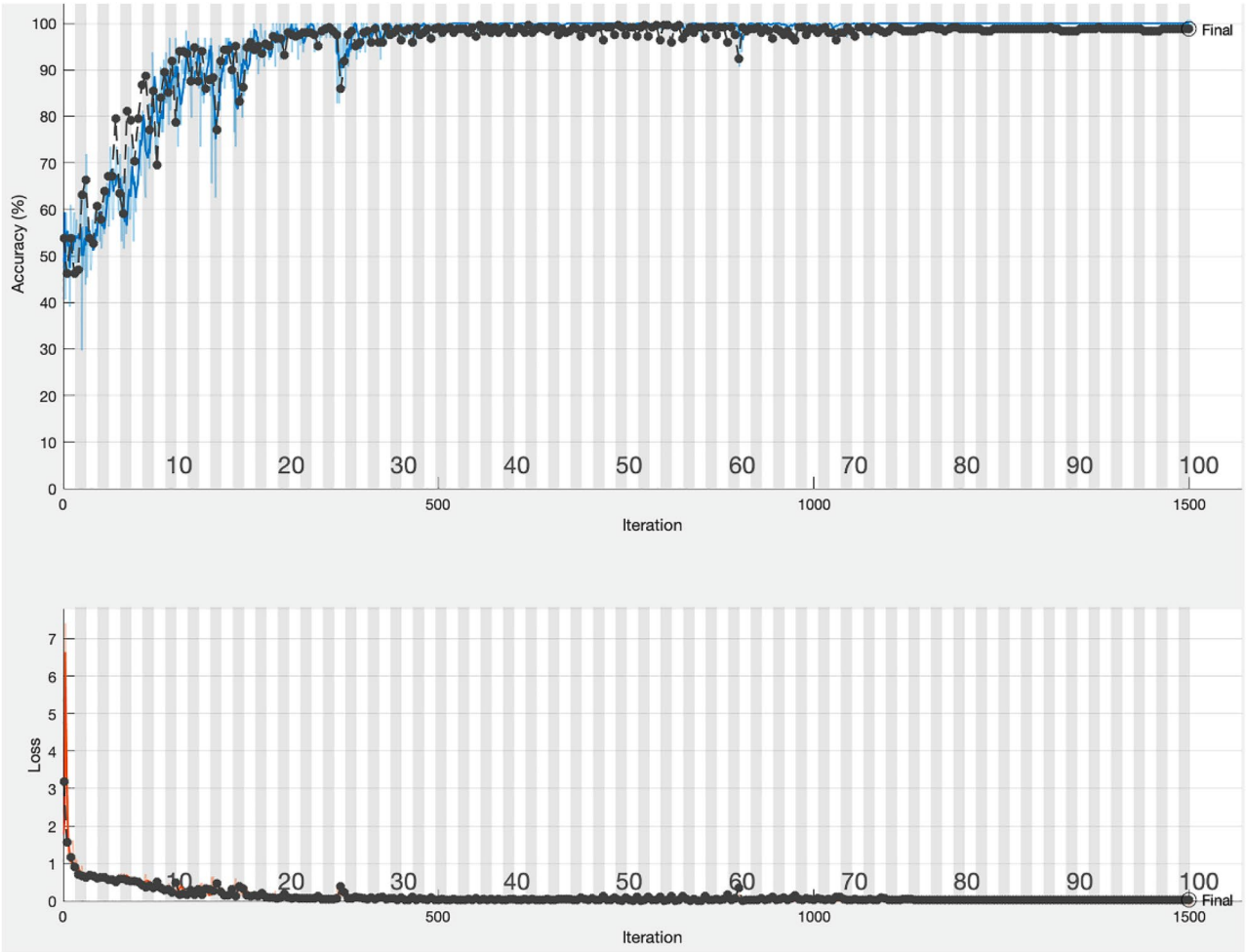

Fig. 4 Training progress of deep learning based on NCCT. The red and black lines indicate the course of training and validation, respectively. The validation accuracy of 98.08% over epoch 100 was used, and the cross-entropy loss curve represents the good fit between a prediction and the ground truth

in 2.4~10% of patients within 24~36 h after thrombolysis and is associated with an increased risk of subsequent death or disability [39], so the timely recognition of early ischemic changes on NCCT is critical for improving stroke outcomes.

In this study, all NCCT images in the stroke group were obtained within 6 h after symptom onset. Using DCNN on the stroke classification achieved higher than 90% accuracy in the model training and test using the institution A dataset, as shown in Table 2. Considering that AlexNet without transfer learning still achieved high accuracy, although more training time was necessary, the accuracy implied that the collected dataset was enough to establish the acute ischemic stroke classification model from a specific scanner. Comparing AlexNet and transferred AlexNet, the transferred parameters were learned from color natural images in ImageNet, which may not be optimized for grayscale NCCT images. Tested by a dataset from institution B (Table 3), although AlexNet trained from scratch had only 60% accuracy, the transferred DCNNs achieved substantial performance (80–85%) and have potential clinical use. The experimental results demonstrate that training DCNN from scratch can be customized for a specific scanner. For example, a system is only applied in a single institution or for a scanner. In another way, if a CAD is used for general purposes, the

Table 2 Performance comparisons of different DCNNs using training and test datasets from institution A

	AlexNet	Transferred AlexNet	Transferred Inception-v3	Transferred ResNet101
Accuracy	97.12%	90.49%	94.62%	95.49%
Sensitivity	98.11%	96.98%	93.98%	94.36%
Specificity	96.08%	83.73%	95.29%	96.67%
AUC	0.9927	0.9895	0.9889	0.9897

AUC area under the receiver operating characteristic curve

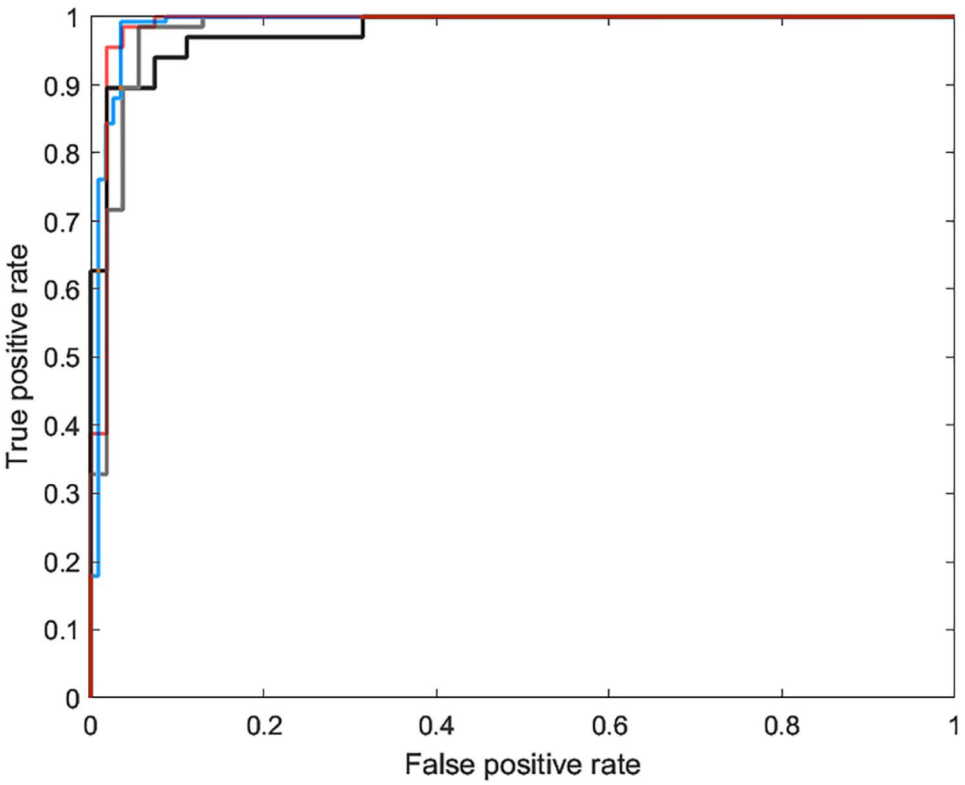

Fig. 5 Comparisons of the receiver operating characteristic curves for each model building including AlexNet (0.9927, red line), transferred AlexNet (0.9895, black line), transferred Inception-v3 (0.9889, green line), and transferred ResNet-101 (0.9897, blue line)

parameters learned from large datasets such as ImageNet would provide more consistent accuracy. The accuracy differences between a customized model and a general model were presented in the experiments. The results show that the highest accuracy and the highest generalizability cannot be obtained simultaneously. To us a DCNN for various scanners, we suggest training a customized model for each scanner. In clinical use, accuracy is the first priority rather than convenience.

In comparison with other CAD systems based on segmentation, edge detection, and feature extraction, previous studies only achieved accuracies and sensitivities of 80~95% [40–42]. RAPID, as an automated ASPECTS in acute MCA stroke, provides an easy, reproducible, and structured method for CT reading [43]. Rutczy'nska et al. [44] proposed a Gaussian mixture model of regional growth for finding the stroke region, but the method was only effective for large lesions and failed to effectively detect early stroke signs. Wu et al. [45] developed an image patch classification-based method to detect ischemic regions using a radiomics-based patch model in CT, and those designs were handcrafted features. Choosing features is time-consuming and operator dependent. The proposed model, which learns relevant features by the training process in DCNN, aids radiologists in focusing on the diagnosis of the ischemic area and subsequent treatment rather than a complicated feature design. Promising results would be helpful in providing diagnostic suggestions in an automatic and consistent way. In particular, the proposed CAD system equipped with an Intel i7-9700 processor, an NVIDIA GeForce GTX 1080 TI graphics card, and 64-GB system memory only spends 0.1 s to determine whether an NCCT slice has stroke. In seconds, a series of brain slices can be evaluated for clinical use. By means of parallelizing and optimizing the implementation, the proposed CAD system will accelerate its practicality. Compared to Food and Drug Administration (FDA)-approved products, StrokeViewer does not provide accuracy or detect lesions for acute ischemic stroke. The use of neural networks for the evaluation model demonstrates that the power and efficiency of DCNNs are undoubted.

This study has some limitations. Although a customized model can be made for a specific scanner, one generalized model is most convenient to use to handle datasets from various scanners. Collecting many datasets remains a challenge. In future studies, we may consider establishing a database with representative images from various

Table 3 Performance comparisons of different DCNNs using an independent test dataset from institution B

	AlexNet	Transferred AlexNet	Transferred Inception-v3	Transferred ResNet101
Accuracy	60.89%	81.77%	85.78%	80.89%
Sensitivity	18.52%	62.04%	75%	61.11%
Specificity	100%	100%	95.73%	99.15%

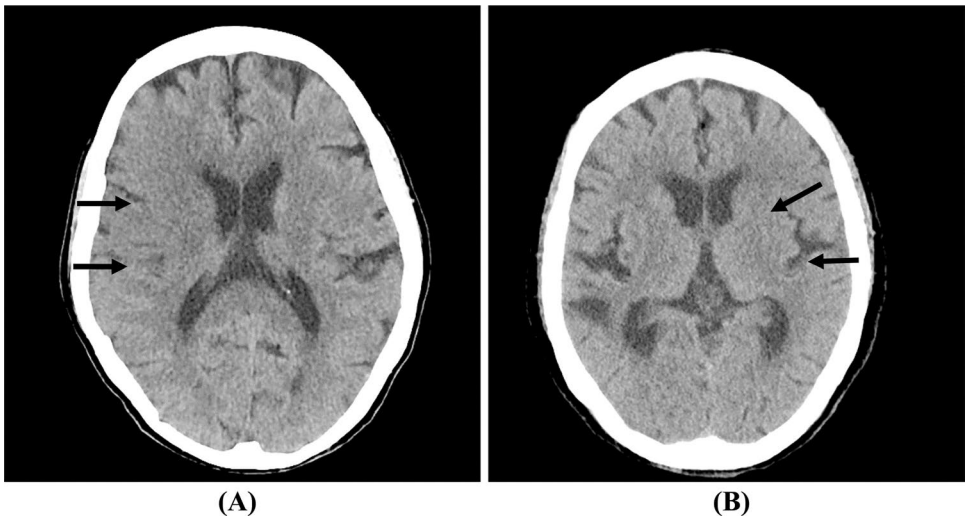

Fig. 6 False-negative cases misclassified by all DCNNs. **a** NCCT shows obscuration and loss of gray–white matter differentiation of the right frontoparietal regions (arrows). **b** NCCT shows subtle hypodensity and effacement in the left basal ganglia and cortical sulci (arrows)

scanners and patients. Size number is an issue only if as the number increases, diversity also increases. Increasing cases similar to the existing training set is not helpful. As long as the dataset is representative, the amount is less important. In addition, more radiologists with substantial clinical experience should be recruited, and whether suggestions from CAD results can improve their accuracy in diagnosing acute ischemic stroke could be explored. To date, the proposed AlexNet model and the transferred DCNN models have performed well in the retrospective diagnosis of acute ischemic stroke using NCCT images.

Conclusion

Based on the developed scheme with DCNN architecture, acute ischemic stroke in NCCT images can be accurately diagnosed with an AUC of > 0.98 for a specific scanner. The accuracy differences between a customized model and a general model were presented. In clinical use, the accuracy of a customized model is more important than its generalizability. Rapid triage and treatment in emergency settings can be achieved with CAD suggestions to radiologists, which will improve treatment quality and result in better patient care.

Funding The authors received financial support from the Ministry of Science and Technology of Taiwan (MOST 108-2221-E-004-010-MY3), the University System of Taipei Joint Research Program (USTP-NTPU-TMU-107-01), and the Mackay Memorial Hospital (MMH-106-150).

Declarations

Conflict of Interest The authors declare no competing interests.

References

1. World Health Organization W, Organization WH. The top 10 causes of death. 2014.
2. Feigin VL, Norrving B, Mensah GA. Global burden of stroke. Circulation research. 2017;120(3):439-48.
3. Krishnamurthi RV, Moran AE, Feigin VL, Barker-Collo S, Norrving B, Mensah GA, et al. Stroke prevalence, mortality and disability-adjusted life years in adults aged 20-64 years in 1990-2013: data from the global burden of disease 2013 study. Neuroepidemiology. 2015;45(3):190-202.
4. Savva GM, Stephan BC, Group AsSVDSR. Epidemiological studies of the effect of stroke on incident dementia: a systematic review. Stroke. 2010;41(1):e41-e6.
5. Phillips LA, Diefenbach MA, Abrams J, Horowitz CR. Stroke and TIA survivors' cognitive beliefs and affective responses regarding treatment and future stroke risk differentially predict medication adherence and categorised stroke risk. Psychology & health. 2015;30(2):218-32.
6. Sacco RL, Adams R, Albers G, Alberts MJ, Benavente O, Furie K, et al. Guidelines for prevention of stroke in patients with ischemic stroke or transient ischemic attack: a statement for healthcare professionals from the American Heart Association/American Stroke Association Council on Stroke: co-sponsored by the Council on Cardiovascular Radiology and Intervention: the American Academy of Neurology affirms the value of this guideline. Stroke. 2006;37(2):577-617.
7. de Castro-Afonso LH, Nakiri GS, Pontes-Neto OM, dos Santos AC, Abud DG. International Survey on the Management of Wake-Up Stroke. Cerebrovascular diseases extra. 2016;6(1):22-6.
8. Hur J, Choi BW. Cardiac CT imaging for ischemic stroke: current and evolving clinical applications. Radiology. 2017;283(1):14-28.
9. Goldstein JH, Denslow SA, Goldstein SJ, Marx WF, Short JG, Taylor RD, et al. Intra-Arterial Therapy for Acute Stroke and the Effect of Technological Advances on Recanalization Findings in a Community Hospital. North Carolina medical journal. 2016;77(2):79-86.
10. Heiferman DM, Li DD, Pecoraro NC, Smolenski AM, Tsimpas A, Ashley Jr WW. Intra-arterial alteplase thrombolysis during mechanical thrombectomy for acute ischemic stroke. Journal of Stroke and Cerebrovascular Diseases. 2017;26(12):3004-8.
11. Kurz K, Ringstad G, Odland A, Advani R, Farbu E, Kurz M. Radiological imaging in acute ischaemic stroke. Eur J Neurol. 2016;23:8-17.

12. Kranz P, Eastwood J. Does diffusion-weighted imaging represent the ischemic core? An evidence-based systematic review. American Journal of Neuroradiology. 2009;30(6):1206-12.
13. von Kummer R, Dzialowski I. Imaging of cerebral ischemic edema and neuronal death. Neuroradiology. 2017;59(6):545-53.
14. Powers WJ, Rabinstein AA, Ackerson T, Adeoye OM, Bambakidis NC, Becker K, et al. 2018 guidelines for the early management of patients with acute ischemic stroke: a guideline for healthcare professionals from the American Heart Association/American Stroke Association. Stroke. 2018;49(3):e46-e99.
15. Muir KW, Buchan A, von Kummer R, Rother J, Baron J-C. Imaging of acute stroke. The Lancet Neurology. 2006;5(9):755-68.
16. Wintermark M, Rowley HA, Lev MH. Acute stroke triage to intravenous thrombolysis and other therapies with advanced CT or MR imaging: pro CT. Radiology. 2009;251(3):619-26.
17. Liu L, Tian Z, Zhang Z, Fei B. Computer-aided detection of prostate cancer with MRI: technology and applications. Academic radiology. 2016;23(8):1024-46.
18. Jalalian A, Mashohor S, Mahmud R, Karasfi B, Saripan MIB, Ramli ARB. Foundation and methodologies in computer-aided diagnosis systems for breast cancer detection. EXCLI journal. 2017;16:113.
19. Virmani J, Kumar V, Kalra N, Khandelwal N. SVM-based characterisation of liver cirrhosis by singular value decomposition of GLCM matrix. International Journal of Artificial Intelligence and Soft Computing. 2013;3(3):276-96.
20. Taşcı E, Uğur A. Shape and texture based novel features for automated juxtapleural nodule detection in lung CTs. Journal of medical systems. 2015;39(5):46.
21. Choi JJ, Kim SH, Kang BJ, Song BJ. Detectability and usefulness of automated whole breast ultrasound in patients with suspicious microcalcifications on mammography: comparison with handheld breast ultrasound. Journal of breast cancer. 2016;19(4):429-37.
22. Cheng PM, Malhi HS. Transfer learning with convolutional neural networks for classification of abdominal ultrasound images. Journal of digital imaging. 2017;30(2):234-43.
23. Gulshan V, Peng L, Coram M, Stumpe MC, Wu D, Narayanaswamy A, et al. Development and validation of a deep learning algorithm for detection of diabetic retinopathy in retinal fundus photographs. Jama. 2016;316(22):2402-10.
24. Esteva A, Kuprel B, Novoa RA, Ko J, Swetter SM, Blau HM, et al. Dermatologist-level classification of skin cancer with deep neural networks. Nature. 2017;542(7639):115.
25. Han SS, Kim MS, Lim W, Park GH, Park I, Chang SE. Classification of the clinical images for benign and malignant cutaneous tumors using a deep learning algorithm. J Invest Dermatol. 2018;138(7):1529-38.
26. Krizhevsky A, Sutskever I, Hinton GE, editors. Imagenet classification with deep convolutional neural networks. Adv Neural Inf Process Syst; 2012.
27. Kim D, MacKinnon T. Artificial intelligence in fracture detection: transfer learning from deep convolutional neural networks. Clinical radiology. 2018;73(5):439-45.
28. Chung SW, Han SS, Lee JW, Oh K-S, Kim NR, Yoon JP, et al. Automated detection and classification of the proximal humerus fracture by using deep learning algorithm. Acta Orthop. 2018;89(4):468-73.
29. Zech JR, Badgeley MA, Liu M, Costa AB, Titano JJ, Oermann EK. Variable generalization performance of a deep learning model to detect pneumonia in chest radiographs: A cross-sectional study. PLoS Med. 2018;15(11):e1002683.
30. Liang G, Zheng L. A transfer learning method with deep residual network for pediatric pneumonia diagnosis. Computer Methods and Programs in Biomedicine. 2019.
31. Szegedy C, Liu W, Jia Y, Sermanet P, Reed S, Anguelov D, et al., editors. Going deeper with convolutions. Proceedings of the IEEE conference on computer vision and pattern recognition; 2015.
32. He K, Zhang X, Ren S, Sun J, editors. Deep residual learning for image recognition. Proceedings of the IEEE conference on computer vision and pattern recognition; 2016.
33. Smajlović D, Sinanović O. Sensitivity of the neuroimaging techniques in ischemic stroke. Medicinski arhiv. 2004;58(5):282-4.
34. Camargo EC, Furie KL, Singhal AB, Roccatagliata L, Cunnane ME, Halpern EF, et al. Acute brain infarct: detection and delineation with CT angiographic source images versus nonenhanced CT scans. Radiology. 2007;244(2):541-8.
35. Prakkamakul S, Yoo AJ. ASPECTS CT in acute ischemia: review of current data. Topics in Magnetic Resonance Imaging. 2017;26(3):103-12.
36. Yong SW, Bang OY, Lee PH, Li WY. Internal and cortical border-zone infarction: clinical and diffusion-weighted imaging features. Stroke. 2006;37(3):841-6.
37. Bal S, Bhatia R, Menon BK, Shobha N, Puetz V, Dzialowski I, et al. Time dependence of reliability of noncontrast computed tomography in comparison to computed tomography angiography source image in acute ischemic stroke. International Journal of Stroke. 2015;10(1):55-60.
38. Demeestere J, Scheldeman L, Cornelissen SA, Heye S, Wouters A, Dupont P, et al. Alberta stroke program early CT score versus computed tomographic perfusion to predict functional outcome after successful reperfusion in acute ischemic stroke. Stroke. 2018;49(10):2361-7.
39. Yan S, Jin X, Zhang X, Zhang S, Liebeskind DS, Lou M. Extensive cerebral microbleeds predict parenchymal haemorrhage and poor outcome after intravenous thrombolysis. J Neurol Neurosurg Psychiatry. 2015:jnnp-2014–309857.
40. Nowinski WL, Gupta V, Qian G, He J, Poh LE, Ambrosius W, et al. Automatic detection, localization, and volume estimation of ischemic infarcts in noncontrast computed tomographic scans: method and preliminary results. Investigative radiology. 2013;48(9):661-70.
41. Tyan Y-S, Wu M-C, Chin C-L, Kuo Y-L, Lee M-S, Chang H-Y. Ischemic stroke detection system with a computer-aided diagnostic ability using an unsupervised feature perception enhancement method. Journal of Biomedical Imaging. 2014;2014:19.
42. Gomolka RS, Chrzan RM, Urbanik A, Nowinski WL. A quantitative method using head noncontrast CT scans to detect hyperacute nonvisible ischemic changes in patients with stroke. Journal of Neuroimaging. 2016;26(6):581-7.
43. Maegerlein C, Fischer J, Mönch S, Berndt M, Wunderlich S, Seifert CL, et al. Automated Calculation of the Alberta Stroke Program Early CT Score: Feasibility and Reliability. Radiology. 2019;291(1):141-8.
44. Rutczyńska A, Przelaskowski A, Jasionowska M, Ostrek G. Method of brain structure extraction for CT-based stroke detection. Information Technologies in Biomedicine: Springer; 2010. p. 133–44.
45. Wu G, Lin J, Chen X, Li Z, Wang Y, Zhao J, et al. Early identification of ischemic stroke in noncontrast computed tomography. Biomed Signal Process Control. 2019;52:41-52.